Transactions, SMiRT-22
San Francisco, California, USA - August 18-23, 2013
Division 2

AN INVESTIGATION OF BOND BEHAVIOR OF LARGE-SIZE STEEL BAR USED IN NUCLEAR CONCRETE CONTAINMENT

Yu-Cheng Kan[1], Kuang-Chih Pei[2], Li-Hwei Chen[3], Bryan Z. Kan[4]

1 Associate Professor , Dept. of Construction Engineering, Chaoyang University of Technology, Taiwan (yckan@cyut.edu.tw)
2 Senior Engineer, Institute of Nuclear Energy Research, Taiwan
3 Ph.D. Candidate, Dept. of Construction Engineering, Chaoyang University of Technology, Taiwan
4 Graduate student, Dept. of Civil Engineering, National Cheng Kung University, Taiwan

ABSTRACT

This research attempts to investigate the bond behavior between concrete and rebar in various sizes (D19, D32, D43 and D57) through the pull-out test that follows to ASTM C234. In the testing program, three concrete mixtures of compressive strengths at 27.4, 34.2 and 41.6 MPa were adopted. And, the bond behavior of concrete with a embedded crack along the rebar is also designated. Acoustic emission (AE) was employed to monitor the crack of concrete during the load test. The test results indicated that the ultimate peak load carrying capacity increased as the steel bar diameter increased. In addition, the ultimate peak load displacement is reduced with increases in steel bar diameter. Under the same concrete strength, the greater the steel bar diameter, the lower the initial crack bond strength and ultimate bond strength. For the same steel bar type, the initial crack bond load bearing capacity and the ultimate bond load bearing capacity increase as the concrete strength increased, but the concrete initial crack bond strength and the ultimate bond strength decreased as steel bar diameter increased. The pullout test showed that when concrete embedded with D57 diameter steel bar reached the ultimate strength, the stress of the steel bar was only approximately 10% to 13% of the yield strength and could not achieve the ultimate strength. In consequence, steel bar with a smaller diameter is recommended for design to achieve higher mechanical efficiency.

INTRODUCTION

Plenty of researches efforts have been conducted in studying the bond behavior of steel rebar and concrete; while rare researches have studied the bond of large-size rebar (D43 and D57) in concrete. Ferguson et al, (1965) have studied the development length for reinforcing bars which varying sizes of rebar including D57. It explored that larger bars embedded in concrete will demonstrate a different bond behavior as that of smaller bars and extra cover did not improve observed widths at service loads for large bars. The current ACI code provides the development length for rebar in concrete for design, instead of bond strength which was adopted to design the nuclear containment in 1970s. However, due to little evidence of bond behavior of large-size rebar in concrete is provided, it is felt significant to make a systematically investigation by a series of tests.

The factors affect the bond between the deformed bar and concrete are chemical adhesion, friction forces and mechanical anchorage of the ribs against the concrete surface. These factors may be implicated in three major subject headings: structural characteristics, bar properties, and concrete properties. The bar properties covered includes bar size and geometry, steel stress and yield strength, and bar surface condition. For a given development length, larger bars achieve higher total bond forces than smaller bars, which is concluded in ACI 408 (2003). It indicated that for a given bonded length, larger bar require larger forces to cause either a splitting or pull-out failures. Orangun (1977) and Darwin (1996) have the same conclusion that the bond force at failure increases more slowly than the bar area, which means that a larger embedment length is needed for a larger bar to fully develop a given bar stress. Parviz

and Choi (1989) also investigated the effects of bar diameter (No.6 to No.10) on the local bond stress-slip relationship and indicated that the bond strength decreases as the bar diameter increases. The drop in bond strength is a linear of bar diameter.

Since the early nuclear power plant were started to constructed from 40 years ago, the codes did not provide rigorous consideration for the detailed design of the concrete containment, in particular, in the bonding problems between steel reinforcement and concrete, resulting in cracks on the surface of containment. This study attempt to explore the mechanical bonding of concrete and various sizes of steel bars through steel bar bonding tests and analyzed the mechanical behavior for concrete and steel bars generating cracks.

Reinforced Concrete Bond Behavior

The basic principle of the reinforced concrete composite material mechanism is that sufficient boundary conditions must exist between the steel reinforcement and the concrete to transfer the acting force between the two; and this transference is provided by the adhesive force at the boundaries of the reinforced concrete. Ribs were added to the surface of the steel reinforcement to enhance the adhesive force and enable the internal acting force to prevent the steel reinforcements from sliding vertically within the concrete. This acting force is called bonding. The ACI Committee 408 defined bond stress as stress that is transferred along the boundary between the steel bars and concrete. The binding force between the concrete and the steel bars changes along the longitudinal direction of the steel bar, which is the shear stress received by the steel bar unit surface area. Therefore, the nature of the boundary between the steel bars and the concrete is very closely related to bond stress. The three general factors that affect bond strength are listed below.

(1) Chemical Adhesion between Steel Bars and Concrete

The cement hydration effects of the concrete produce strong cement gel chemical reactants that generate a portion of the bond stress through the interface adhesion effect between the two components. When the components are under low stress, bond resistance is provided by the chemical cohesive force. If the steel bars slide, the limited bond resistance immediately disappears.

(2) Friction between the Steel Bars and Concrete

The impedance force caused by the roughened or uneven steel bar surface during the relative parallel motion is known as friction or frictional force. When chemical adhesion is lost and minor sliding occurs between the steel bars and the concrete, bond strength is provided by the frictional force and the interlock caused by the concrete's effect on the steel bars' flanged surface.

(3) Interlock between the Steel Bars and Concrete

The interlock bearing stress between the steel bar ribs and the concrete is even more critical when further sliding of the two occur. As the steel bars begin to slide, adhesion force is lost and bonding strength is provided by the acting force and frictional effects of the concrete on the steel bar ribs. When the steel bars slide, the limited bonding resistance is lost. Therefore, chemical adhesion is not the main source of bonding strength. When chemical adhesion is lost and minor sliding of the steel bars and concrete occurs, bond strength is provided by the frictional force and bearing stress caused by the concrete's effect on the flanged surface of the steel bars. This bearing stress becomes even more critical as the steel bars and the concrete further slide.

Bond Failure Types

Two failure models are commonly seen during steel bar and concrete pullout tests. In the first model, when the steel bar protection level is sufficiently thick, concrete tends to break or shear horizontally between the steel bar ribs. Bond failure results in the steel bar being pulled out of the concrete, causing the concrete to have holes instead of splitting cracks. In the second model, when the

steel bar protection level is insufficiently thick, the concrete surrounding the steel bar shows splitting crack failure with several crack surfaces from the pressure and pushing caused by steel bar surface ribs.

Acoustic Emissions Monitoring For Concrete

Several fundamental differences exist between acoustic emission technology and other non-destructive techniques: (1) acoustic emissions can be used to monitor the entire dynamic process or the cracking behavior (e.g., the extension and expansion of cracks); it does not monitor static defects; (2) crack signals result directly from the crack itself and external stress waves are not input to detect defects; and (3) the load history of the structure can be observed through this process, and the possibilities for damage processes can be determined during observation.
The application and development of the acoustic emission method for homogeneous materials has matured considerably. However, more data for developing the relationship between heterogeneous concrete materials and mechanical behavior characteristics is required. During the material experiment process, the acoustic emission method can be used to monitor the emitted sounds to establish the relationship between acoustic emissions, microscopic mechanisms, and mechanical characteristics to (1) analyze the relationship between material cracking, deformation, and mechanical behavior; and (2) establish a broad acoustic emission signals database. A study by Minfess (1982) has stated that during pure concrete compression tests, the number of acoustic emissions passing the threshold increased as the load increased. At approximately 80% to 90% of the ultimate load, sound inside the concrete increased and accelerated, indicating that cracks are forming in the concrete.

EXPERIMENTAL PROGRAM

This study explores the mechanical bond behavior between concrete and steel bars of varying sizes, and analyzed the mechanical behavior that occurs between concrete and steel bars creating cracks. In addition, acoustic emission signal change monitoring was employed to predict the initial crack point and peak load points.

Table 1 Concrete mixture proportions

Mixture	W/C	Cement	Water	Aggregate	Sand	SP**
A	0.62	299*	185	1132	751	0.99
B	0.52	353	184	1125	716	1.18
C	0.45	404	183	1033	753	1.62

*Unit of weight is kg per cubic meter.

**Super-plasticizer

Specimen Design

Three mix designs were used in this test as shown in Table 1. A pullout test cube was designed in which four sizes of steel bars and cylindrical specimens were embedded, for a total of twelve groups. The size of the cubic specimen was affected because the diameter of the D43 and D57 steel bars is larger than that used in general construction. In addition, the concrete cover for nuclear facilities generally exceeds 10 cm, which also was designed as a 260 mm × 260 mm × 260 mm. While the cubic specimens were

produced, cylindrical specimens (ϕ100 mm × 200 mm) were also created to determine the compression strength of the concrete.

Pullout Test

For this study, we referenced the ASTM C234 pullout test method to examine the bond characteristics between the steel bars and the concrete; consequently, three cubic specimens for each bar size were fabricated. All of the concrete specimens were cured after 28-day curing period. A rubber gasket was placed at the contact surface between the steel pullout frame and the concrete specimen to ensure uniform strength transmission and to prevent the stress concentration phenomenon. In addition, an LVDT was erected to measure the relative displacement between the steel bars and concrete, and four acoustic emission monitoring probes were used to monitor the initial crack load and the peak load. The test configuration is shown in Figs. 1 and 2. All of the pull-out tests were conducted on an MTS test system.

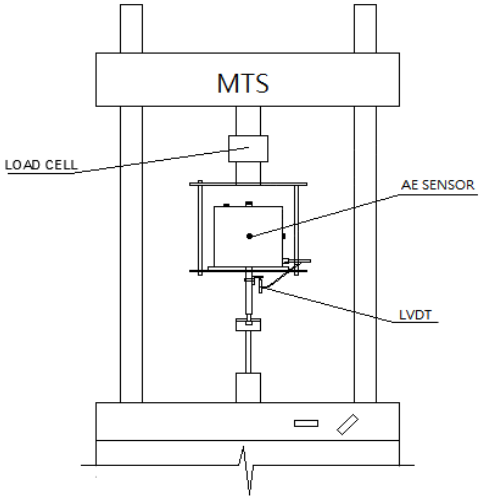

Figure 1 Configuration of pull-out test

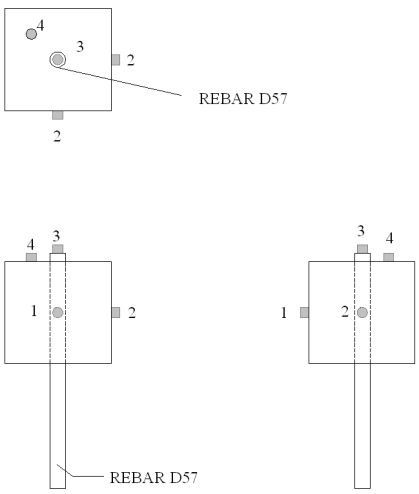

Figure 2 Locations of AE sensors

Displacement control was conducted in automatic mode. The loading rate was controlled at 0.01 mm/s, and the acoustic emission monitoring system was used to record sound signals inside the concrete simultaneously. The data acquisition controller was used to record the MTS added load strength and LVDT displacement values. These data were to be used in subsequent analysis and discussion. The experiment was concluded when the increased load caused structural failure of the concrete specimen.

Acoustic Emissions Monitoring for Bond Stress Tests

As the specimens bore stress, friction and cracking occurred in the reinforced concrete, creating sound waves detectable by probes of the acoustic emissions monitoring device. The acoustic emissions capture device and a computer system then represented the sound waves as a signal graph. The corresponding load to the peak position of the acoustic emission signal density was considered the initial cracking load. This indicates that, after cracking, the displacement and friction events of the reinforced concrete boundary significantly increased.

RESULT AND DISCUSSION

In this study, the bond stress behavior of large-scale reinforced concrete including the various stress stages in concrete and rebar were investigated. The bond properties of concrete were summarized in Tables 2. The concrete strength designed in this study were 27.4 MPa, 34.3 MPa, and 41.2 MPa, corresponding to mixtures A, B and C.

Table 2 Bond property of concrete

f_c' MPa	Rebar	Loading properties						
		P_c, kN	P_u, kN	P_c/P_u%	U_c, MPa	$U_c / \sqrt{f_c'}$	U_u, MPa	$U_u / \sqrt{f_c'}$
27.4	D19	54.5	92.8	59	3.51	0.64	5.98	1.09
	D32	59.8	118.0	51	2.29	0.42	4.52	0.82
	D43	68.0	124.6	55	1.94	0.35	3.55	0.65
	D57	75.0	138.7	54	1.61	0.29	2.98	0.54
34.2	D19	55.7	99.2	56	3.59	0.61	6.39	1.09
	D32	57.6	106.5	54	1.47	0.25	4.08	0.69
	D43	62.9	114.9	55	1.96	0.33	3.27	0.56
	D57	74.3	135.5	55	1.60	0.27	2.91	0.50
41.2	D19	67.4	105.9	64	4.34	0.63	6.82	0.99
	D32	76.1	130.6	58	2.91	0.42	5.00	0.73
	D43	87.2	153.2	57	2.48	0.36	4.36	0.63
	D57	109.2	178.5	61	2.35	0.34	3.84	0.56

Figure 3 shows typical bond test load-slip curves of the steel bars of varying size types. The embedded D57 steel bar pullout specimen had the greatest ultimate peak load bearing capacity, followed by the D43, D32, and D19 steel bar specimens. The embedded D57 steel bar pullout specimen was observed to have the lowest ultimate peak load displacement, followed by the D43, D32, and D19 steel bar specimens. In addition, the load position change diagram indicated that after each steel bar specimen had reached the ultimate peak load, another peak was formed after a slight decline. However, this peak was smaller than the ultimate peak load and called the secondary peak load. This phenomenon was most significant for the embedded D57 steel bar pullout specimen, followed by the D43, D32, and D19 steel bar specimens.

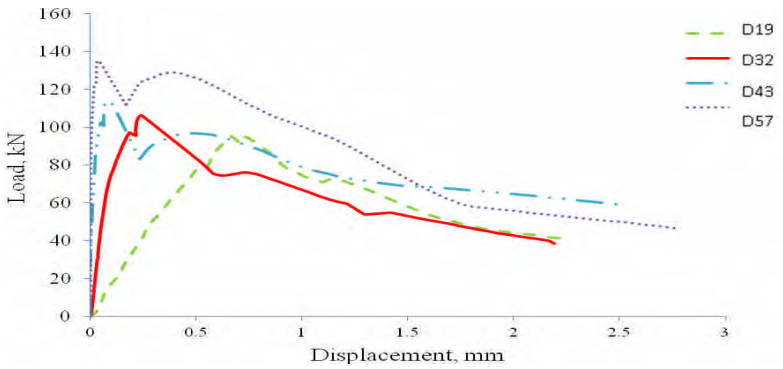

Figure 3 Load-displacement curves of pull-out test

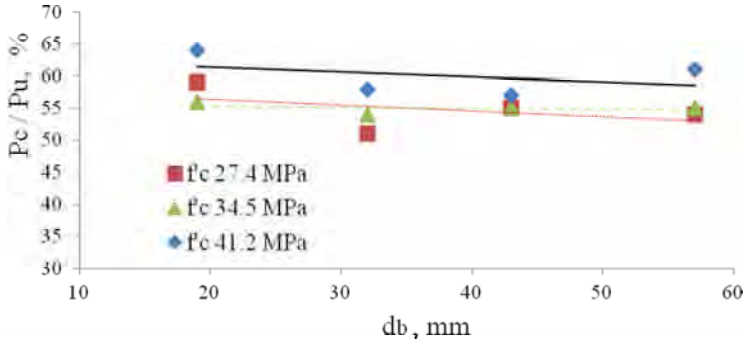

Figure 4 Initial cracking load versus diameter of steel

Figure 4 showed that the specimens' initial cracking load and ultimate load ratio P_c/P_u ranging from 51% to 64%, regardless of diameter of steel bar. However, the higher the concrete strength, the closer the initial cracking load was to the ultimate strength; and the greater the diameter of the steel bar, the more frequently initial cracking occurred at the low-load stage. Figures 5 indicated that the initial

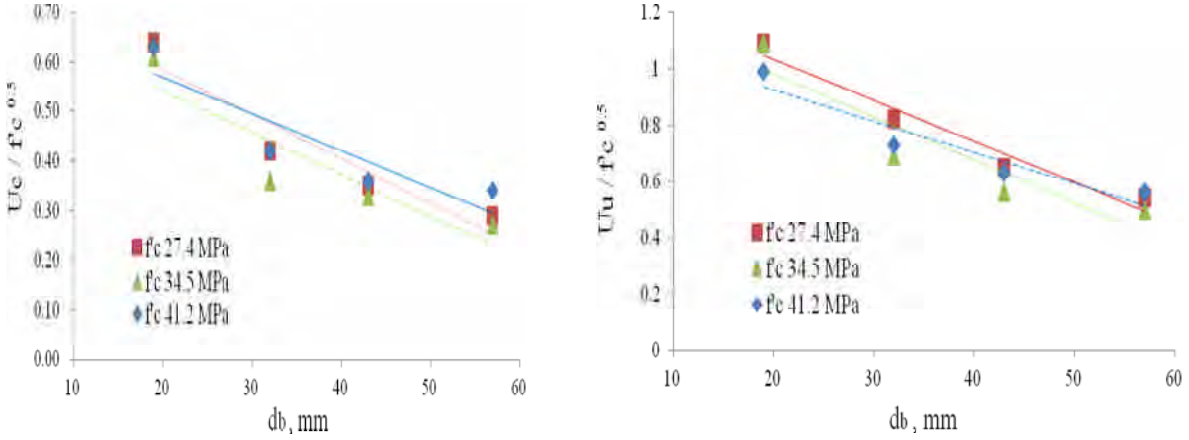

(a) Initial cracking load (b) Ultimate load

Figure 5 Initial cracking load and ultimate load versus diameter of steel bar

cracking strength and ultimate bond strength decreased as the diameter of the steel bars increased. Nominal bond strength, in terms of $U_u / \sqrt{f_c'}$. The decline rates for the three different strengths of concrete specimens with increases in the diameter of steel bars were roughly identical.

The bond properties of steel bars were shown in Table 3. In Fig. 6 the steel bar stress at bond failure indicated that the larger the steel bar diameter, the lower the steel bar stress. The D57, D43, D32, and D19 steel bars showed similar results with three concrete strengths. Among them, the stress percentage results for concrete with strengths of 27.4 MPa and 34.5 MPa were almost identical. In addition, the steel bar stress for the concrete with a strength of 41.2 MPa tended to be larger than those for concrete with strengths of 27.4 MPa and 34.5 MPa, which indicated that the stronger the concrete strength, the better the bond or cohesive force between the steel bars and the concrete, and the greater stress the steel bar could bear.

Table 3 Bond property of rebar

f_c' MPa	Rebar	Loading properties				
		$f_{sc,}$ MPa	$f_{peak,}$ MPa	$f_{y,}$ MPa	$f_{sc}/f_{y,}$ %	$f_{peak}/f_{y,}$ %
27.4	D19	192	328	469	41	70
	D32	74	147	483	15	30
	D43	47	86	442	11	19
	D57	29	54	439	7	12
34.2	D19	197	350	469	42	75
	D32	69	132	483	14	27
	D43	47	79	442	11	18
	D57	29	53	439	7	12
41.6	D19	238	374	469	51	80
	D32	95	162	483	20	34
	D43	60	106	442	14	24
	D57	43	70	439	10	16

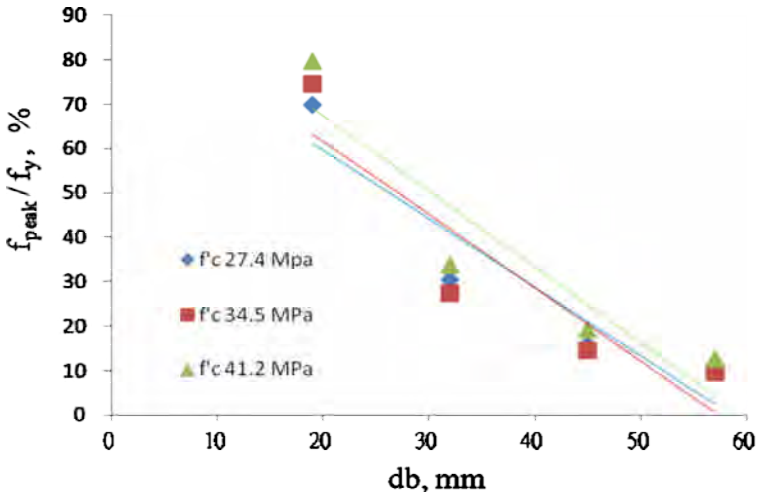

Figure 6 Steel bar stresses at bond failure

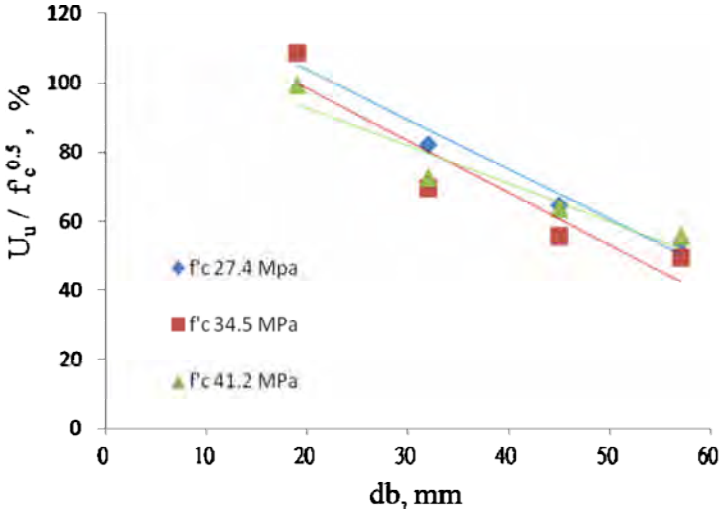

Figure 7 Concrete stresses at bond failure

Figures 7 indicated ultimate bond stress state for the specimens that the concrete bond stress, in terms of Uu / √fc' for varying compressive strengths. Obviously, the higher the compressive strength behaved larger the bond strength of concrete.

An interaction between steel bar and concrete stresses at bond failure for various compressive strengths are demonstrated in Figures 8 to 10. It can be seen that the stress of D19 diameter steel bars can reach approximately 41% to 51% of yield strength at the initial cracking stage. While the steel bar stress in that stage for D32, D43, and D57 was 14% to 20%, 9% to 11%, and 5% to 8% of yield strength, respectively. Regardless of the concrete strength, the ratio of rebar bond strength to the yielding strength for steel bars with D19, D32, D43, and D57 diameters was 70% to 80%, 27% to 34%, 14% to 19%, and 10% to 13% of yield strength, irrespectively. Because when bond pullout stress for the concrete achieved an ultimate limit, no yielding occurred, the concrete demonstrated splitting failure behavior.

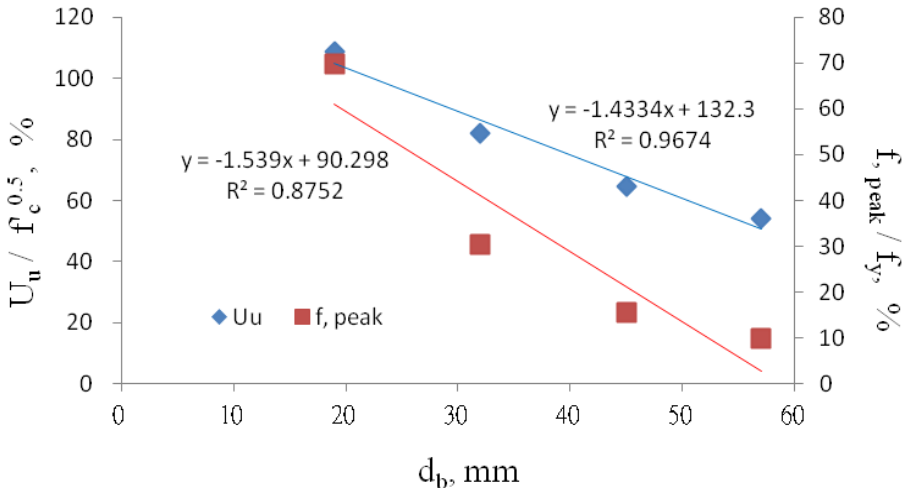

Figure 8 Stress ratio of steel and concrete at bond failure for fc' = 27.4 MPa

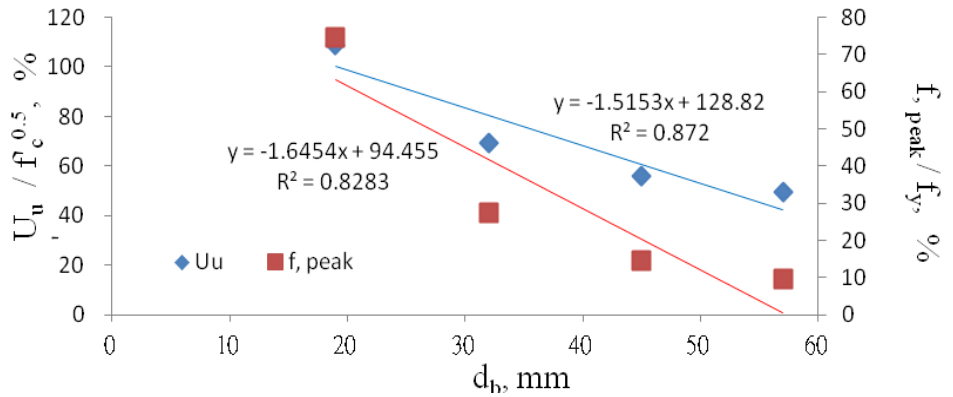

Figure 9 Stress ratio of steel and concrete at bond failure for fc' = 34.5 MPa

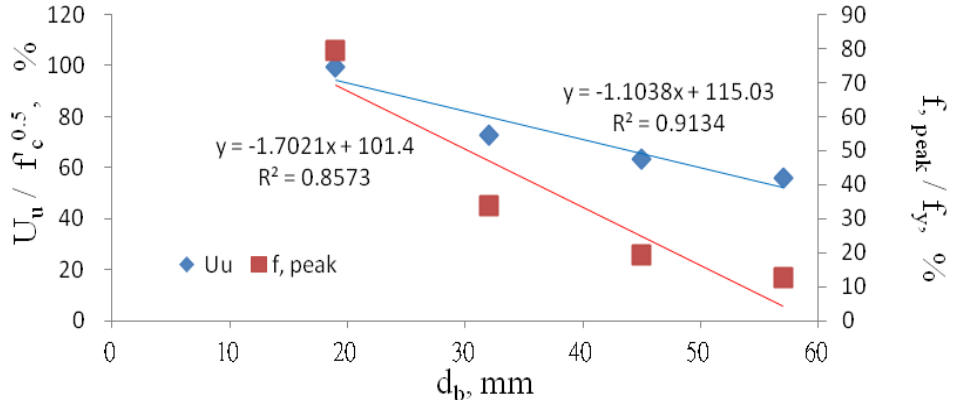

Figure 10 Stress ratio of steel and concrete at bond failure for fc' = 41.2 MPa

CONCLUSION

In this study, the analysis and results can be summarized into the following conclusions.

- Based on the typical bond test load position change for steel bars of various types, the ultimate peak load carrying capacity increased as the steel bar diameter increased. In addition, the ultimate peak load displacement is reduced with increases in steel bar diameter. Under the same concrete strength, the greater the steel bar diameter, the lower the initial crack bond strength and ultimate bond strength.
- For the same steel bar type, the initial crack bond load bearing capacity and the ultimate bond load bearing capacity increase as the concrete strength increased, but the concrete initial crack bond strength and the ultimate bond strength decreased as steel bar diameter increased.
- The residual strength of completely cracked specimens increases as the diameter of the steel bars increase. A similar trend was observed for all steel bars except D32. Generally, the residual strength was approximately 65% to 88% regardless of the bar size.
- The pullout test showed that when concrete embedded with D43 and D57 diameter steel bars reached the ultimate strength, the steel bars' ultimate bond stress was only approximately 8% to 16% of their yield strength and could not achieve the target ultimate strength. Therefore, we recommend that steel bars with a smaller diameter be used as replacements to reduce the thickness of the protection layer and enable the steel bars to achieve higher mechanical efficiency.

REFERENCES

Ferguson, P. M., Breen, J. E. and Thompson, J. N. (1965)"Pullout Test on High strength Reinforcing Bar," Part 1, *ACI Journal*, Vol. 62, No. 8, pp. 933-950.

ACI 408,"Bound and Development of Straight Reinforcing Bars in Tension", American concrete Institute, Farmington Hills, Mich.2003, pp1-15.

Orangun,C. O., Jirsa, J. O. and Breen, J. E. (1977) "A Re-evaluation of Test Data on Development Length and Splices," *ACI Journal*, Vol. 74, No.3, pp. 114-122.

Darwin, D.; McCabe, S.L.; Idun, E. K.; and Schoenekase, S. P.,"Development Length Criteria; Bars Not Confined by Transverse Reinforcement," *ACI structural Journal*, V.89, No.6, Nov.-Dec.1992, pp. 709-720.

Soroushian, P., Choi, K. B.(1989） "Local bond of deformed bars with different diameters in confined concrete," *ACI Structural Journal*, Vol.86, No.2,pp.217-222.

Ezeldin, A. S. and Balaguru, P. N. (1989)"Bond behavior of normal and high-strength fiber reinforced concrete," *ACI Materials Journal*, Vol. 86, No.5, pp. 515-524.

Rehm, G. "The Basic Principles of the Bond between Steel and Concrete," Translation NO.134, Cement and Concrete Association, London, pp.90（1968）

Gergely, P. "Splitting Cracks Along the Main Reinforcement in Concrete Members" Report to Bureau of Public Roads U.S. Department of Transportation, Cornell University, Ithaca, N.Y., pp.90（1969）

Soroushian, P., Mirza, F. and Alhozaimy, A.（1994）"Bonding of confined steel fiber reinforced concrete to deformed bars," *ACI Materials Journal*, Vol.91, No.2, pp.144-149.

Kan,Y.C., Pei,K.C., Lin, D.W.(2007) "Monitoring real-time fracture within reinforced concrete under the load test using acoustic emission recording technique," *Proceeding*, 19th SMiRT, Toronto, August 12-17.

Minfess, S. (1982) "Acoustic emission and ultrasonic pulse velocity of concrete," *International Journal of Cement Composites and Lightweight Concrete*, Vol. 4, No. 3, pp. 173-179.